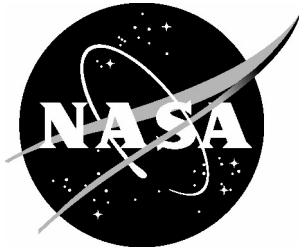# The Influence of Clocking Angle of the Projectile on the Simulated Impact Response of a Shuttle Leading Edge Wing Panel

Karen E. Jackson and Edwin L. Fasanella
U.S. Army Research Laboratory
Vehicle Technology Directorate
Langley Research Center, Hampton, Virginia

Karen H. Lyle and Regina L. Spellman
Langley Research Center, Hampton, Virginia

Since its founding, NASA has been dedicated to the advancement of aeronautics and space science. The NASA Scientific and Technical Information (STI) Program Office plays a key part in helping NASA maintain this important role.

The NASA STI Program Office is operated by Langley Research Center, the lead center for NASA's scientific and technical information. The NASA STI Program Office provides access to the NASA STI Database, the largest collection of aeronautical and space science STI in the world. The Program Office is also NASA's institutional mechanism for disseminating the results of its research and development activities. These results are published by NASA in the NASA STI Report Series, which includes the following report types:

- TECHNICAL PUBLICATION. Reports of completed research or a major significant phase of research that present the results of NASA programs and include extensive data or theoretical analysis. Includes compilations of significant scientific and technical data and information deemed to be of continuing reference value. NASA counterpart of peer-reviewed formal professional papers, but having less stringent limitations on manuscript length and extent of graphic presentations.

- TECHNICAL MEMORANDUM. Scientific and technical findings that are preliminary or of specialized interest, e.g., quick release reports, working papers, and bibliographies that contain minimal annotation. Does not contain extensive analysis.

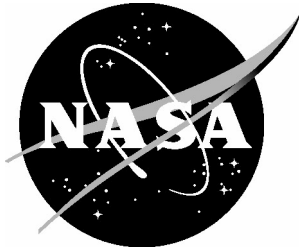- CONTRACTOR REPORT. Scientific and technical findings by NASA-sponsored contractors and grantees.

- CONFERENCE PUBLICATION. Collected papers from scientific and technical conferences, symposia, seminars, or other meetings sponsored or co-sponsored by NASA.

- SPECIAL PUBLICATION. Scientific, technical, or historical information from NASA programs, projects, and missions, often concerned with subjects having substantial public interest.

- TECHNICAL TRANSLATION. English-language translations of foreign scientific and technical material pertinent to NASA's mission.

Specialized services that complement the STI Program Office's diverse offerings include creating custom thesauri, building customized databases, organizing and publishing research results ... even providing videos.

For more information about the NASA STI Program Office, see the following:

- Access the NASA STI Program Home Page at *http://www.sti.nasa.gov*

- E-mail your question via the Internet to help@sti.nasa.gov

- Fax your question to the NASA STI Help Desk at (301) 621-0134

- Phone the NASA STI Help Desk at (301) 621-0390

- Write to:
  NASA STI Help Desk
  NASA Center for AeroSpace Information
  7121 Standard Drive
  Hanover, MD 21076-1320

The Influence of Clocking Angle of the Projectile on the Simulated Impact Response of a Shuttle Leading Edge Wing Panel

Karen E. Jackson and Edwin L. Fasanella
U.S. Army Research Laboratory
Vehicle Technology Directorate
Langley Research Center, Hampton, Virginia

Karen H. Lyle and Regina L. Spellman
Langley Research Center, Hampton, Virginia

March 2005

The Influence of Clocking Angle of the Projectile on the Simulated Impact Response of a Shuttle Leading Edge Wing Panel

Karen E. Jackson and Edwin L. Fasanella
US Army Research Laboratory, VTD
Hampton, VA

Karen H. Lyle and Regina L. Spellman
NASA Langley Research Center
Hampton, VA

Abstract

An analytical study was conducted to determine the influence of clocking, or rotation, angle of a foam projectile impacting a space shuttle leading edge wing panel. Four simulations were performed using LS-DYNA, a commercial nonlinear explicit transient dynamic finite element code. The shuttle wing leading edge panels are fabricated of multiple layers of reinforced carbon-carbon (RCC) material. The RCC material was represented using Mat 58 in LS-DYNA, which is a material property designation that can be used for laminated composite fabrics. During the study, simulations were performed of a 2-in. x 7-in. x 11.88-in. rectangular-shaped foam block, weighing 0.23-lb., impacting RCC Panel 9 on the top surface (location 104). The material properties of the foam were input using Mat 83 in LS-DYNA. For each of the four simulations, the impact velocity was 1,000 ft/s (12,000 in/s) along the Orbiter X-axis. The foam blocks were rotated about their longitudinal axis such that in two of the models the foam impacted on a corner, in one model the foam impacted the panel initially on the 2-in.-long edge, and in the last model the foam impacted the panel on the 7-in.-long edge. The simulation results are presented as contour plots of first principal infinitesimal strain and time history plots of contact force and internal and kinetic energy of the foam and RCC panel. Significant differences in the amount of damage to the RCC panel were observed, indicating that the clocking angle of the projectile is an important parameter in determining the damage threshold.

Introduction

Following the Space Shuttle Columbia disaster on February 1, 2003 and during the subsequent investigation by the Columbia Accident Investigation Board (CAIB), various teams from industry, academia, national laboratories, and NASA were requested by Johnson Space Center (JSC) Orbiter Engineering to apply "physics-based" analyses to characterize the damage threshold of the shuttle thermal protection system (TPS) tile and Reinforced Carbon-Carbon (RCC) material, for high-speed foam impacts. The forensic evidence from the Columbia debris eventually led investigators to conclude that the breach to the shuttle TPS was caused by a large piece of External Tank (ET) foam that impacted and penetrated the lower portion of a left-wing leading edge panel, shown in Figure 1. As a result, NASA authorized a series of tests that were performed at

Southwest Research Institute (SwRI) to characterize the impact response of the leading edge RCC panels.

Recommendation 3.3-2 of the CAIB report [1] requests that NASA initiate a program to improve the impact resistance of the wing leading edge. The second part of the recommendation is to …"determine the actual impact resistance of current materials and the effect of likely debris strikes." For Return-to-Flight (RTF), a team consisting of personnel from NASA Glenn Research Center (GRC), NASA Langley Research Center (LaRC), and Boeing Philadelphia was given the following task: to develop a validated finite element model of the shuttle wing leading edge capable of accurately predicting the threshold of damage from debris including foam, ice, and ablators for a variety of impact conditions. Since the CAIB report was released, the team has been developing finite element models of the RCC leading edge panels; executing the models using LS-DYNA [2], a commercial nonlinear explicit transient dynamic finite element code; conducting detailed material characterization tests to obtain dynamic material property data; and, correlating the LS-DYNA analytical results with experimental data obtained from impacts tests onto RCC panels. Some of the early results of this research are described in References 3-7.
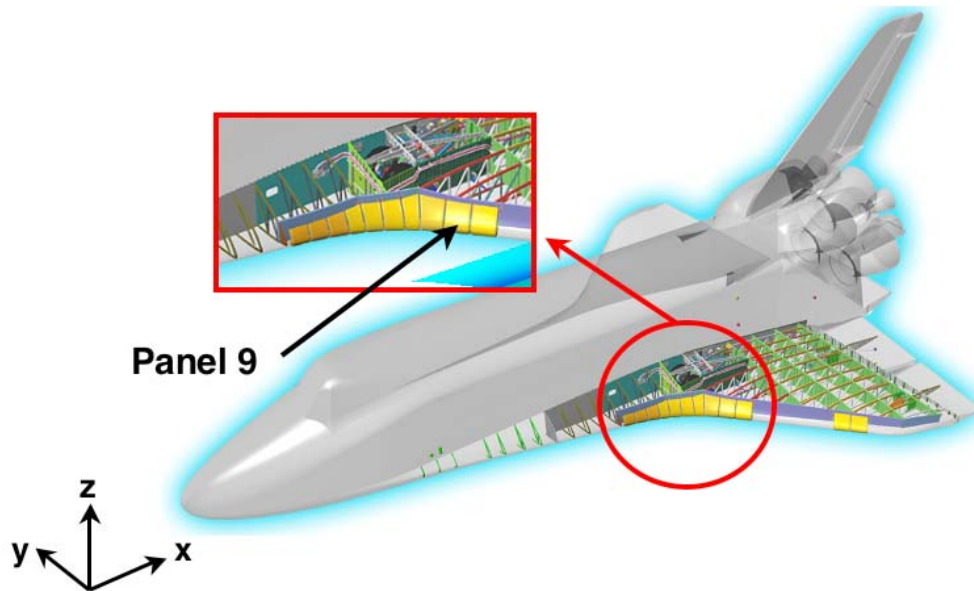

Figure 1. Drawing of the left wing area of the space shuttle.

This paper documents an analytical study that was performed as part of the larger RTF program. The purpose of the study was to examine the influence of rotation, or clocking, angle of a foam projectile impacting space shuttle leading edge wing Panel 9. The foam projectile was assigned the same material properties as the BX-250 foam used on the shuttle ET. The simulations were performed such that the foam projectile impacted the top surface (location 104) of the shuttle leading edge Panel 9 at a velocity of 1,000 ft/s along the Orbiter X-axis. The location of Panel 9 on the left wing of the shuttle is highlighted in Figure 1. During the fall of 2003, three tests were performed at SwRI using BX265 foam blocks impacting onto RCC Panel 9. BX265 foam is a replacement

for BX250 foam and does not require the Freon blowing agent. While the finite element model was originally developed to generate analytical predictions for correlation with experimental data obtained from the SwRI tests, the focus of this study is strictly analytical. A description of the finite element models and comparisons of predicted structural deformations and time-history responses are presented in the following sections of the paper.

Model Description

A side view of the RCC Panel 9 model with the four different foam projectiles is shown in Figure 2. All of the foam blocks are included in this figure to better visualize the different clocking angles. Note that the foam projectiles labeled "Model 1" and "Model 3" impact the panel on the corner of the block, while the one labeled "Model 2" impacts the panel in the middle of the 7-in. edge, called the long edge, of the foam and the one labeled "Model 4" impacts the panel in the middle of the 2-in. edge, called the short edge. It should be noted that Models 1 and 3 and Models 2 and 4 are oriented such that they are perpendicular to one another, respectively. The Panel 9 model was discretized using 57,414 quadrilateral shell elements that were assigned material properties representative of RCC. The panel model consisted of 24 different parts including the panel midsection, two bottom flanges, two side ribs, a doubler region, and twelve filled bolt-holes. Most of these parts are labeled in an exploded view of Panel 9, shown in Figure 3.
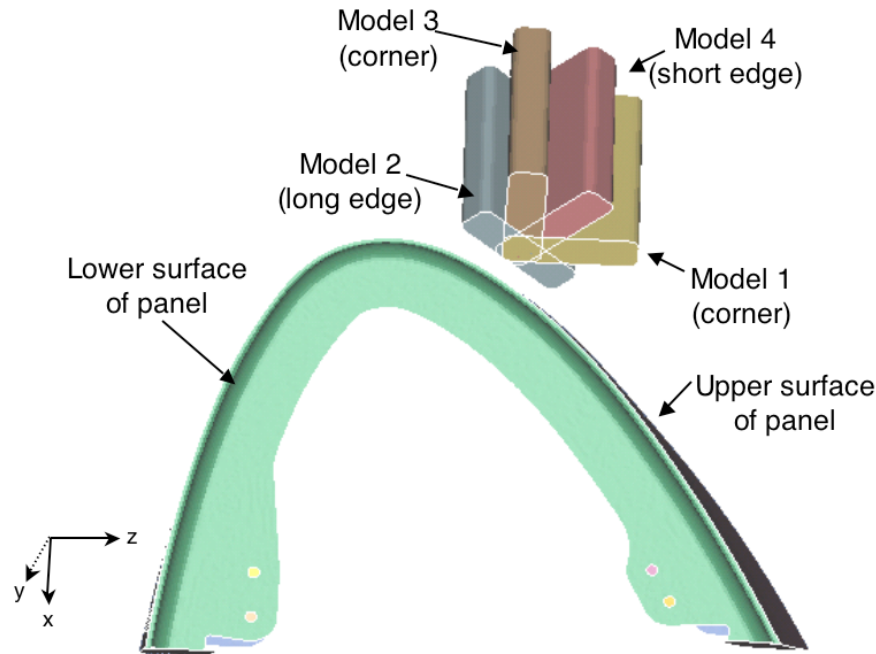

Figure 2. Foam projectiles and shuttle RCC Panel 9 model.

The location on the panel at which the foam impact occurs is identified as location 104, as shown in Figure 4. The location numbers, shown in Figure 4, were used as arbitrary designations by the analysis team. This figure shows a side view schematic of the panel only, without ribs or bottom flanges and several impact locations are identified that have

been studied previously as part of the RTF program. Location 104 is located just above the apex of the panel on the upper surface. As a reminder, while the CAIB investigation found that the shuttle Columbia accident was caused by foam striking the lower leading edge wing panels, this investigation is focused on foam impacts to the upper surface of the panel. This parametric study is part of a larger RTF analytical investigation to characterize the impact damage threshold of the entire RCC panel.
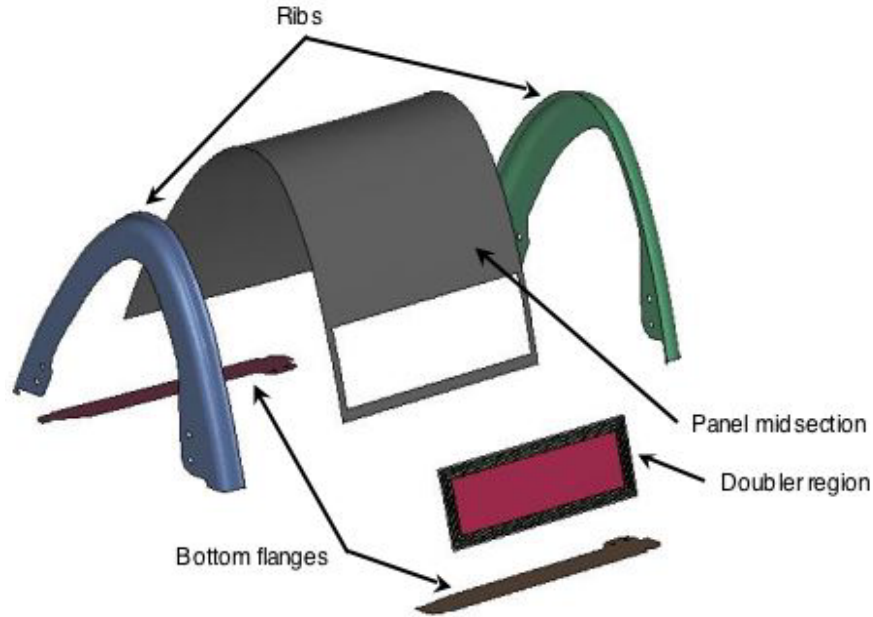

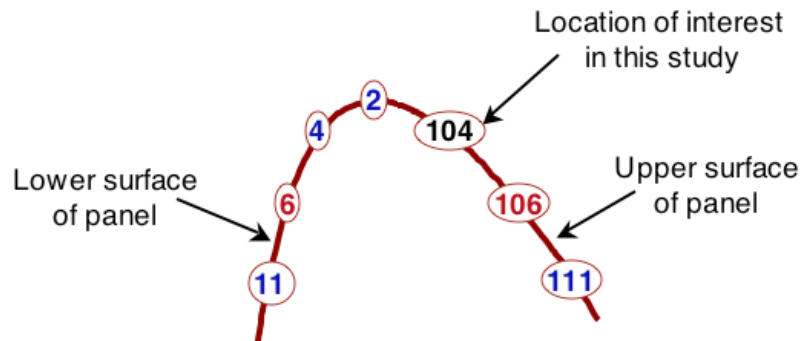Figure 3. Exploded view of Panel 9 with parts labeled.

Figure 4. Side view schematic of panel showing foam impact location 104.

The four models that were executed as part of the clocking angle study are shown individually in Figure 5. Model 1 is depicted on the top left showing the foam block impacting the panel such that the corner of the block initially impacts the top surface of the panel at location 104. For Model 2, shown on the top right of the figure, the foam block impacts the panel at location 104 on the middle of the 7-in., or long, edge. In comparison with the foam block shown in Model 1, the foam block in Model 2 has been rotated clockwise about its longitudinal axis by 45° and then repositioned such that the mid-edge impact of the foam occurs at the same location (104) on the panel as the previous model. For Model 3, the foam projectile has again been rotated by 45° about its

4

longitudinal axis and then repositioned such that the corner of the foam block initially impacts the panel at location 104. Finally, for Model 4, the foam is again rotated by 45° about its longitudinal axis and then repositioned such that the middle of the 2-in., or short, edge of the foam impacts the panel at location 104. As a result of this procedure, all of the foam blocks impact the panel initially at the same location (104).
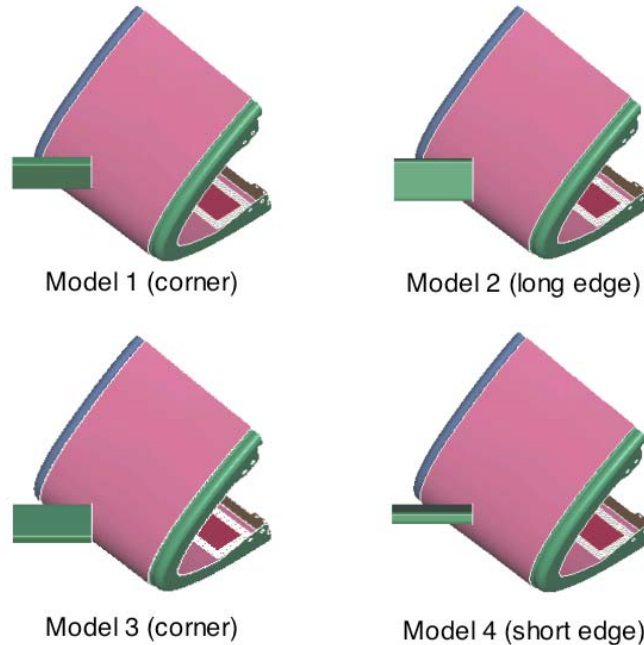

Figure 5. Four foam impact models onto shuttle Panel 9.

The quadrilateral shell elements representing the panel midsection, the two ribs, and the two bottom flanges were assigned RCC material properties using material type 58, MAT_LAMINATED_COMPOSITE_FABRIC. These parts were modeled as a 19-ply laminated composite fabric with the fibers in each layer oriented in the 0°/90° direction. The doubler region is also modeled using quadrilateral shell elements that are assigned to seven different parts. These parts are also modeled using material type 58; however, the number of plies in the RCC doubler varies from a minimum of 20 to a maximum of 38.

Average degraded RCC material properties were used in the Mat 58 material property card. Prior testing of RCC material shows that it is much stiffer and stronger in compression than in tension, thus requiring a bimodular material model. Also, the stiffness and strength of pristine RCC material are significantly higher than flight-conditioned material. Consequently, the term 'degraded' refers to the fact that flight-conditioned material properties were used. RCC also exhibits considerable variability in material response and it is common to see a band or range of curves used to describe the maximum, average, and minimum tensile and/or compressive responses. For this study, the term 'average' means that the average curve was chosen for input.

In the actual RCC Panel 9 tests performed at SwRI, bolts were used to support and constrain the panel at the bolt-hole locations. To account for the constraint provided by the bolts in the model, the bolt-holes were represented using 0.1-in.-thick shell elements

that were assigned rigid material properties using material type 20 MAT_RIGID. These elements were constrained from translational motion in the x-, y-, and z-directions using the BOUNDARY_PRESCRIBED_MOTION_RIGID card in LS-DYNA.

The finite element model of the BX-250 foam projectile had overall dimensions of 2.0 x 7.0 x 11.88-in. and was discretized using hexagonal solid elements having a nominal element edge length of 0.2-in. for a total of 21,889 solid elements. The foam block represented a single part in the LS-DYNA model, making the total number of parts in the model equal to 25. The foam block weighed 0.23-lb.

The material properties of the BX-250 foam were represented using material type 83 MAT_FU_CHANG_FOAM with MAT_ADD_EROSION in LS-DYNA. The erosion card is added to allow for element failure in the foam constitutive model. The experimental foam material responses were input into the model using the DEFINE_CURVE command in LS-DYNA. The responses were obtained from testing of foam components that was performed at NASA GRC and LaRC. These tests were conducted to determine the influence of strain rate on the compressive response of the foam material. Results for two strain rates, 0.01 s^{-1} and 25 s^{-1}, are plotted in Figure 6. The material response data are plotted only up to 200-psi stress to aid in visualization of the differences caused by strain rate; however, the stress data at strain values approaching 1 are 70,000 psi and higher. The stress-strain response of the BX-250 foam, shown in Figure 6, is typical of other foam materials in that it exhibits a linear response at low strains, and as crushing begins a "knee" occurs in the response. Then, as stable crushing continues, the stress increases gradually until the cells within the foam begin to compact. As compaction initiates and continues, the stress increases dramatically for relatively small increases in strain. As shown in Figure 6, the influence of strain rate is to increase the stress at which the knee occurs, to increase the stress during stable crushing, and to lower the strain at which compaction begins. A tensile failure stress of 86-psi was assigned to the foam, based on test data.

All of the nodes in the foam model were assigned an initial velocity of 1,000 ft/s (12,000 in/s) in the Orbiter X-direction, which is defined from the nose to the tail of the shuttle. A CONTACT_ERODING_NODES_TO_SURFACE was specified between the panel midsection and the foam in the model. For this contact, the panel midsection was designated the master surface, and the foam was the slave. Due to the eroding feature of this contact definition, a foam element may fail, or erode, and the contact will be picked up by the next element.

For this analytical study, simulations were performed for four different clocking angles of the foam projectile. For these four simulations, the foam and panel models were assigned the same material properties, initial velocity conditions, and contact definitions. Thus, only the clocking angle of the foam was varied. Each model was executed for 0.004 s (4 ms) of simulation time using LS-DYNA Version 970 on a single-processor Linux-based Hewlett Packard workstation x4000.
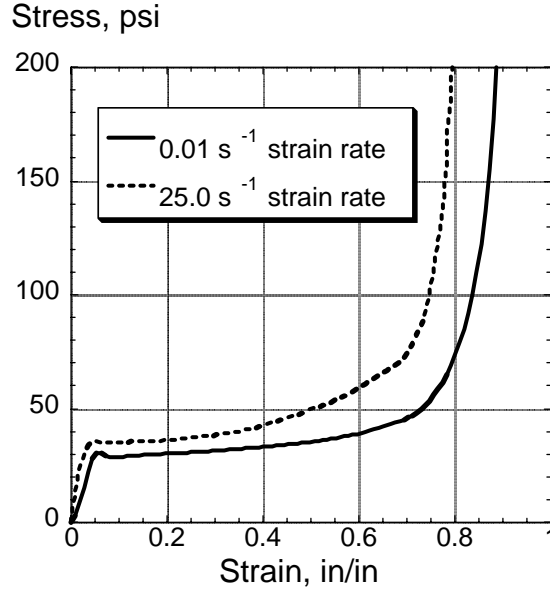
Figure 6. Compressive material properties of BX-250 foam for two different strain rates.

Simulation Results

The results of the analytical study are presented in two main categories: contour plots of first principal infinitesimal strain of Panel 9 at four discrete time steps and time history plots of contact force, and internal and kinetic energy of the panel and foam.

Contour Plots
Contour plots of first principal infinitesimal strain in the panel at 1, 2, 3, and 4 ms are presented in Figures 7-10, respectively. These plots were created for a fixed fringe level ranging between 0.0 to 0.006 in/in. This range was selected because the approximate failure strain of RCC is 0.006 in/in. The panels are depicted as viewed from above, without the foam projectile. As shown in Figures 7-10, the amount of damage to the panel increases progressively for each successive time interval. At 1.0 ms, no shell elements in any of the models have failed. However, the contour plots in Figure 7 show areas of varying size and shape that are colored for the maximum strain level, thus indicating that element failure is imminent. In particular, Model 2 shows a large area on the panel that is shaded for the maximum strain level.

By 2.0 ms, all of the panels exhibit some element failures indicating the initial formation of a crack or hole in the panel, see Figure 8. The amount and location of damage is different for each panel. For example, model 1 exhibits only a small hole created by the failure of a few shell elements. Conversely, model 2 shows a large crack that runs parallel to the rib/panel interface. Likewise, model 3 shows the formation of a large crack that runs parallel to the rib/panel interface and is located close to the rib. Model 4 exhibits a slightly skewed crack, running generally perpendicular to the rib/panel interface. Obviously, the location and amount of initial damage to the panel is different, depending on the rotation angle of the foam projectile.
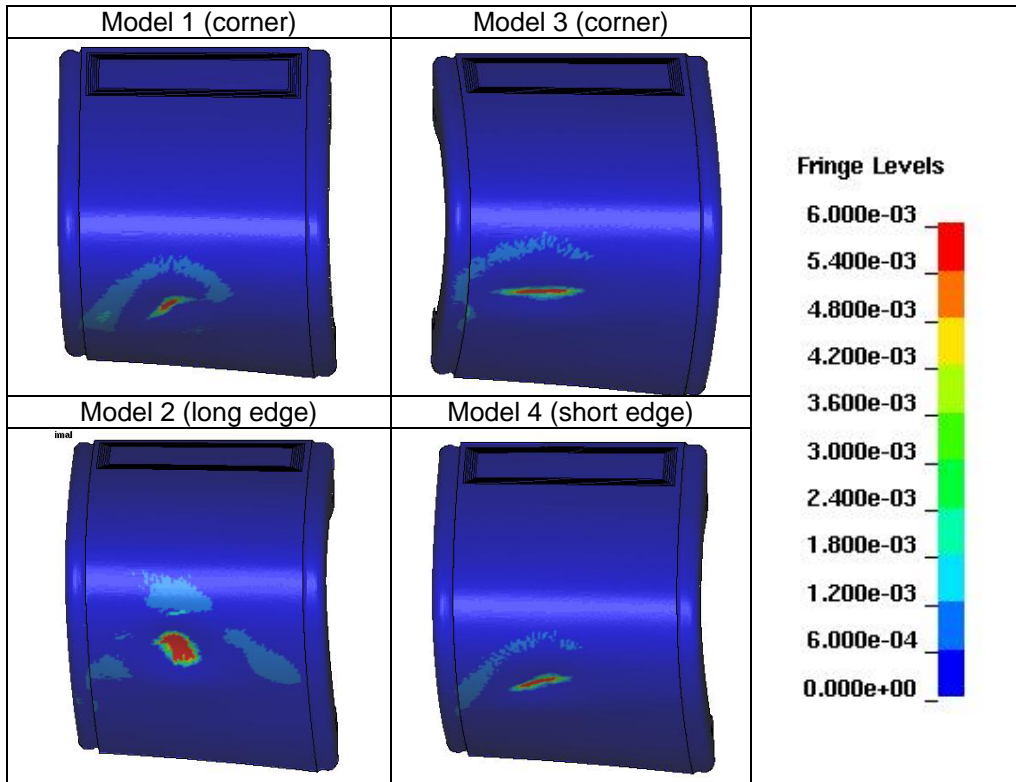
7

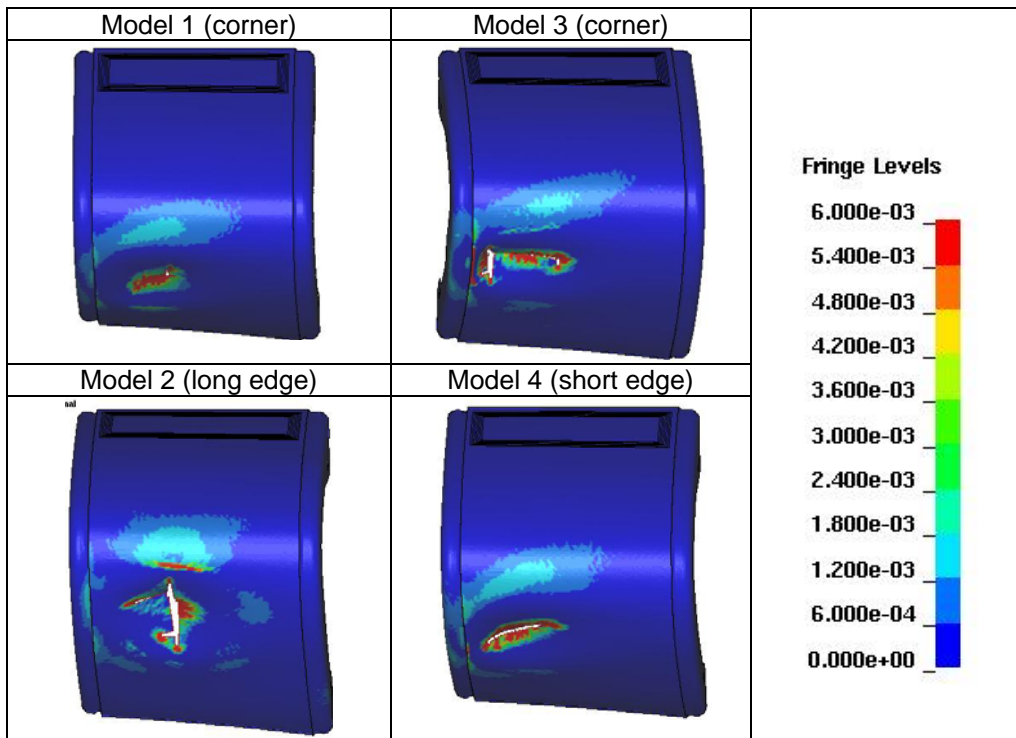Figure 7. Comparison of contour plots of first principal infinitesimal strain at 1.0 ms.

Figure 8. Comparison of contour plots of first principal infinitesimal strain at 2.0 ms.

By 3.0 ms, the damage has increased significantly in all of the panels except for model 1 which stills shows a very small hole of nearly the same size as for the previous time step. In models 2 and 3, the cracks shown at 2 ms have now grown into large holes, as shown in Figure 9, with additional cracks emanating from the holes. For model 4, the skewed crack has continued to grow, now in a direction parallel to the rib-panel interface.

By 4.0 ms, the damage in the model 1 panel has stabilized with no additional element failures, as shown in Figure 10. However, the other three models indicate that the amount of damage to the panel continues to increase. Of these three, model 4 shows the least increase in damage. Both of the panels in models 2 and 3 exhibit large gaping holes, as shown in Figure 10.
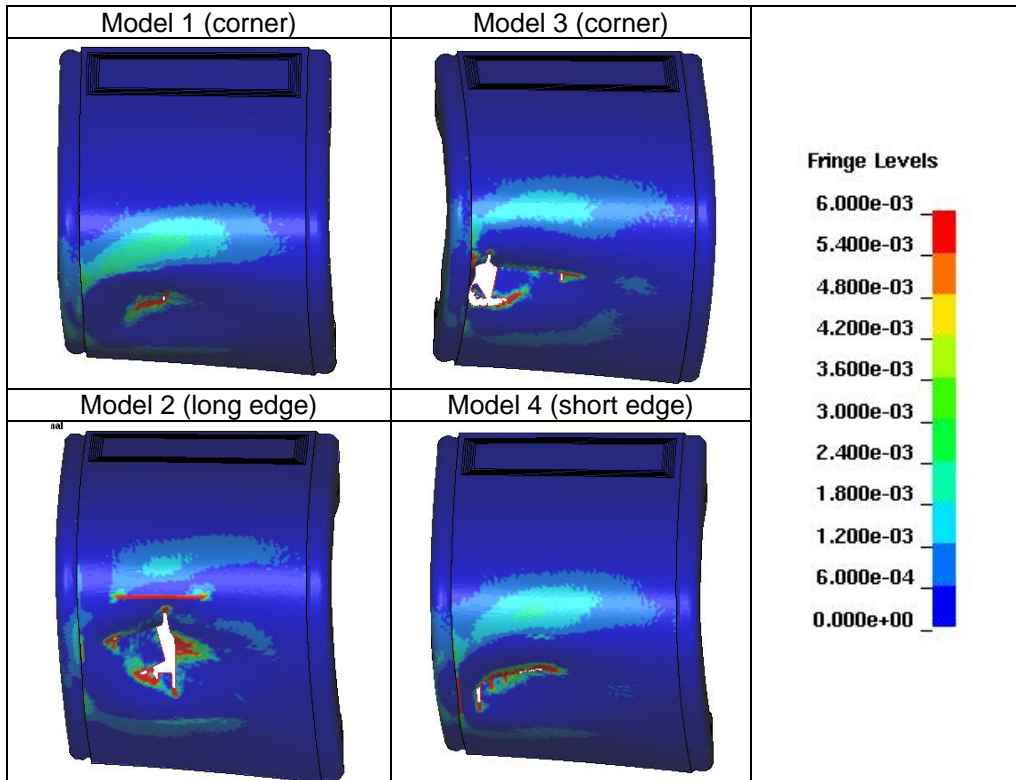

Figure 9. Comparison of contour plots of first principal infinitesimal strain at 3.0 ms.

Close-up views of the failed areas of the four panels are shown in Figure 11. It can be difficult to characterize the size and extend of damage to the panels. The method chosen for this study was to estimate the area enclosed by the failed elements and those elements that appear to be close to failure, based on the contour plot data. The results of this analysis are documented in Table 1. It can be seen that the Model 2 and 3 panels sustained the greatest amount of damage, and the damaged areas were determined to be 39.76- and 38.6-in^2, respectively, for these two models. Thus, based on these results, it appears that the model 2 simulation, in which the long edge of the foam block initially impacts the panel, is the most severe condition, followed closely by the model 3 case, in which the corner of the foam impacts the panel.
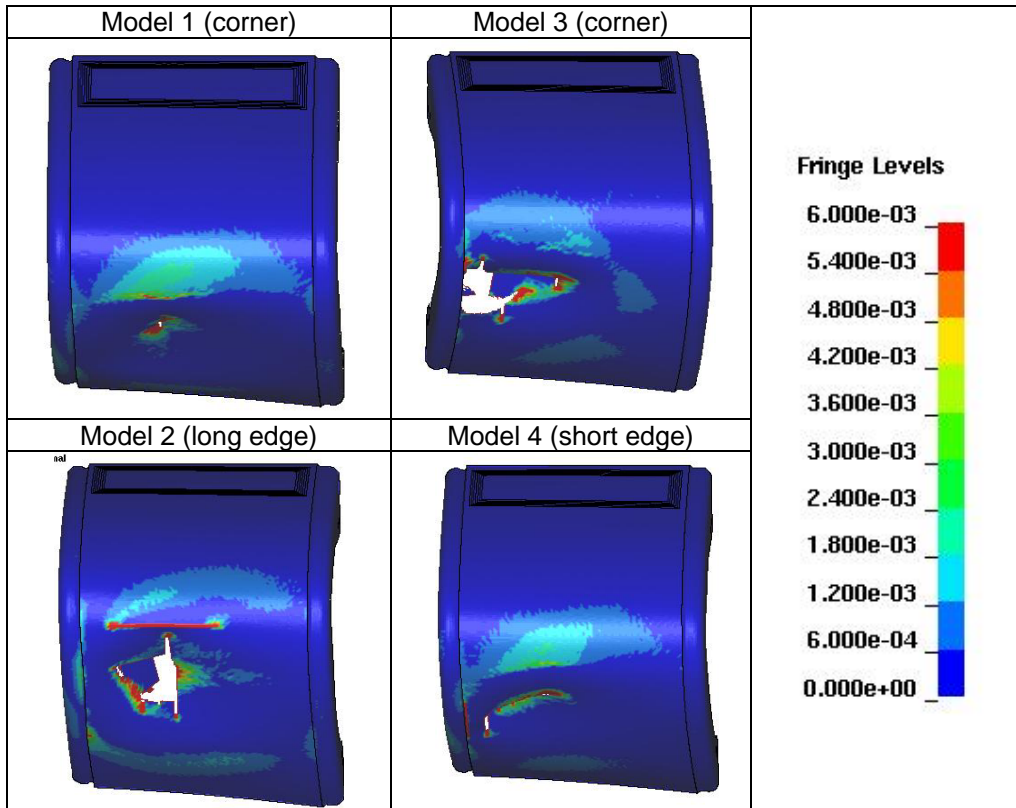
Model 1 (corner)	Model 3 (corner)	
		Fringe Levels
		6.000e-03
		5.400e-03
		4.800e-03
		4.200e-03
		3.600e-03
Model 2 (long edge)	Model 4 (short edge)	3.000e-03
		2.400e-03
		1.800e-03
		1.200e-03
		6.000e-04
		0.000e+00

Figure 10. Comparison of contour plots of first principal infinitesimal strain at 4.0 ms.

Model 1 (corner)	Model 3 (corner)
Model 2 (long edge)	Model 4 (short edge)
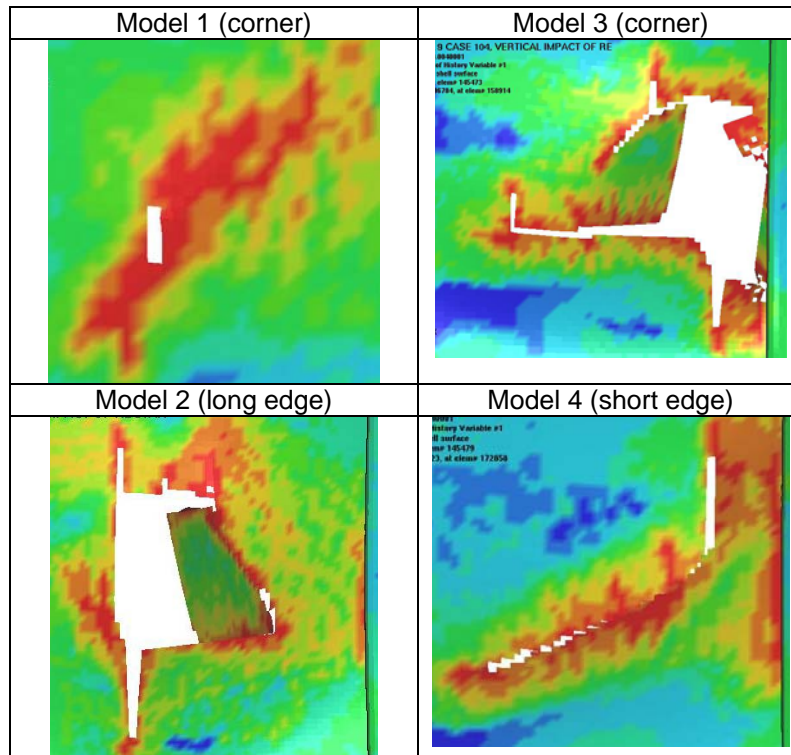
Figure 11. Close-up views of the contour plots of first principal strain at 4.0 ms.

<u>Time History Plots</u>
Comparisons of time history responses of contact force and internal and kinetic energy of the foam and panel for the four clocking angle simulations are presented in this section of the paper. The time history responses were obtained as direct output of the post-processing and the curves have not been filtered or modified. The contact force results from models 1 and 2 are shown in Figure 12 (a) and the results from models 3 and 4 are shown in Figure 12 (b). This convention is used for all of the subsequent time history comparisons. Each of the force time history responses shown in Figure 12 was integrated to obtain the area under the curve, which is the impulse. The values of impulse for each curve are listed in the plot legend and in Table 1

(a) Model 1 and 2 results. (b) Model 3 and 4 results.
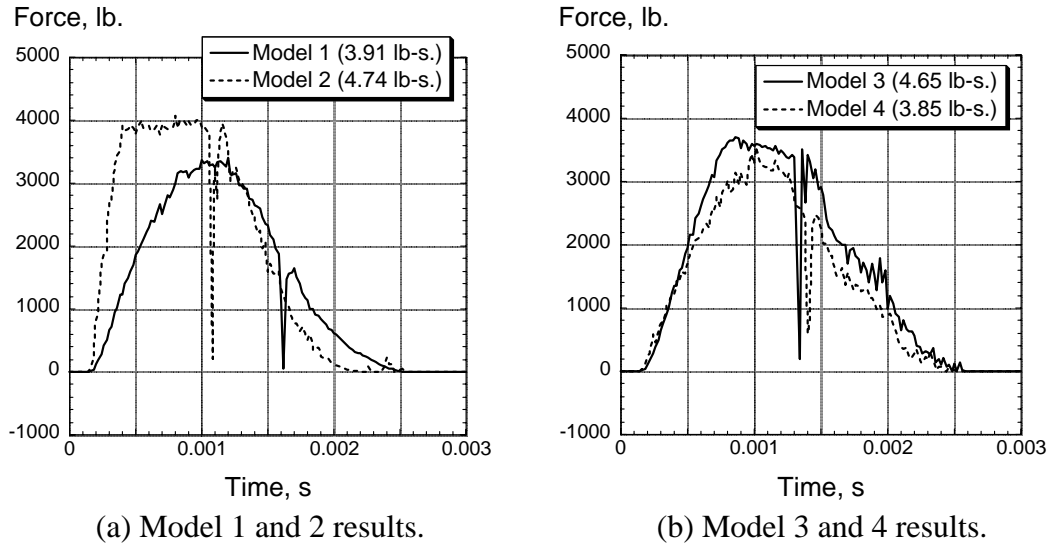
Figure 12. Time history responses of contact force. Note: the impulse of each curve is shown in the parenthesis in the plot legend.

The contact force responses differ in peak magnitude, time of occurrence of the peak, and overall shape of the curves, as shown in Figure 12. The peak values range in magnitude from a maximum of 4,000-lb. for model 2 to a minimum of 3,300-lb. for model 1. In general, three of the four responses exhibit a sinusoidal shape; however, the shape of the contact force response for model 2 is different. This curve rises quickly to a maximum value of 4,000-lb., remains constant at that value for a duration of about 0.00075 s, and then drops off gradually to zero force. It can be seen that all of the force responses exhibit a large downward spike that occurs during the latter portion of the response. These spikes can be attributed to numerical anomalies in the contact algorithms. Later, the contact algorithms were changed and these anomalies were eliminated. The impulse values range from a maximum of 4.74 lb-s for model 2 to a minimum of 3.85 lb-s for model 4. These values are important in that they reflect the relative change in momentum that occurs during the impact.

The internal energy time history responses of the foam are shown in Figure 13, which follows the same convention as used in Figure 12. It is interesting to note that the internal energy responses exhibited by models 2 and 3 are similar in magnitude and

11

shape. Also, the responses of models 1 and 4 are similar in magnitude and shape, yet the two sets of curves are different from one another.   In both cases, models 1 and 2 exhibit a higher magnitude response when compared with models 4 and 3, respectively.

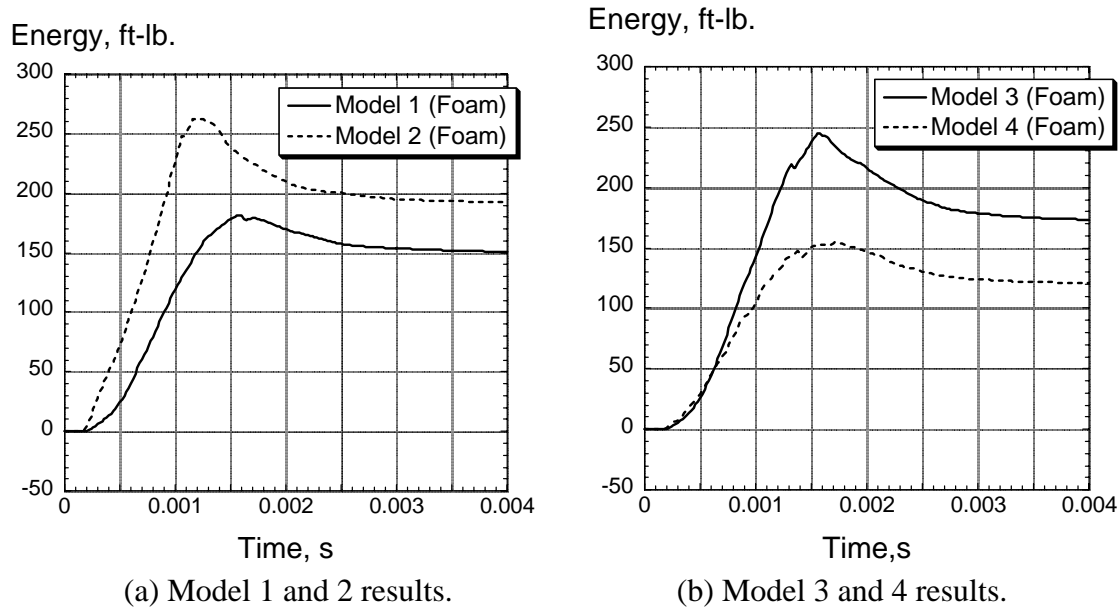(a) Model 1 and 2 results.   (b) Model 3 and 4 results.

Figure 13. Time-history responses of the internal energy of the foam.

The kinetic energy time history responses of the foam are shown in Figure 14. Three of the four kinetic energy responses exhibit the same overall shape with a gradual reduction in kinetic energy up to approximately 0.002 second, followed by a leveling off of the response. For example, three of the four curves have a kinetic energy value of 2,500 ft-lb at 0.001 s. However, the response of the model 2 is quite different form the other curves. The response curve for this model falls off dramatically and has begun to level off by 0.0015 s. For comparison, the kinetic energy value at 0.001 second for this model is 2,100 ft-lb, 400 ft-lb less that the other three models. It is also interesting to note that the four models have slightly different values of kinetic energy remaining at the end of the simulation at 0.004 s. The model that exhibits the largest change in kinetic energy of the foam (initial value minus the end value) is model 3.

The internal energy time-history responses of the RCC portion of the models are shown in Figure 15. For these two plots and the kinetic energy plots shown in Figure 16, the total energies of all of the parts of the model were summed, except that the foam was excluded. Thus, the RCC responses reflect the behavior of the entire panel 9 model, and not just the response of the upper surface of the model only. The RCC internal energy responses of the four simulations exhibit the same trend as seen in the previous plots. Three of the four responses are similar in shape and magnitude, but the model 2 response is different. In this case, the internal energy response of model 2 is much greater in magnitude than the other three curves and, whereas the other curves level off at a maximum value, the response of model 2 continues to increase without leveling off. The maximum values of internal energy of the RCC were determined from the plots and are

listed in Table 1.   The fact that the internal energy of the RCC for model 2 is considerably higher than the other models indicates that the strain energy in the panel is also much higher, resulting in more global deformation of the panel.
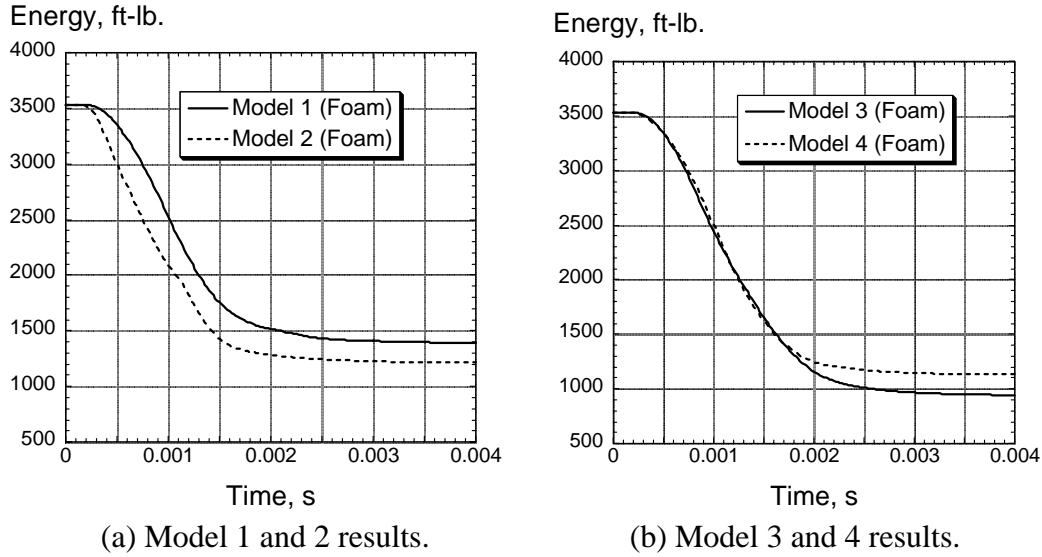
Energy, ft-lb.

(a) Model 1 and 2 results.

Energy, ft-lb.

(b) Model 3 and 4 results.

Figure 14. Time-history responses of the kinetic energy of the foam.

Finally, the kinetic energy time history responses of the RCC model are shown in Figure 16.   These curves are generally sinusoidal in shape initially, reach a peak value, and then gradually decrease in magnitude.   Once again, the trend is for three of the curves to exhibit similar responses, while the response of model 2 is different.   In this case, the model 2 exhibits the highest peak value of kinetic energy, indicating that a higher percentage of the kinetic energy of the projectile is converted into kinetic energy of the RCC.

Energy, ft-lb.

(a) Model 1 and 2 results.

Energy, ft-lb.

(b) Model 3 and 4 results.
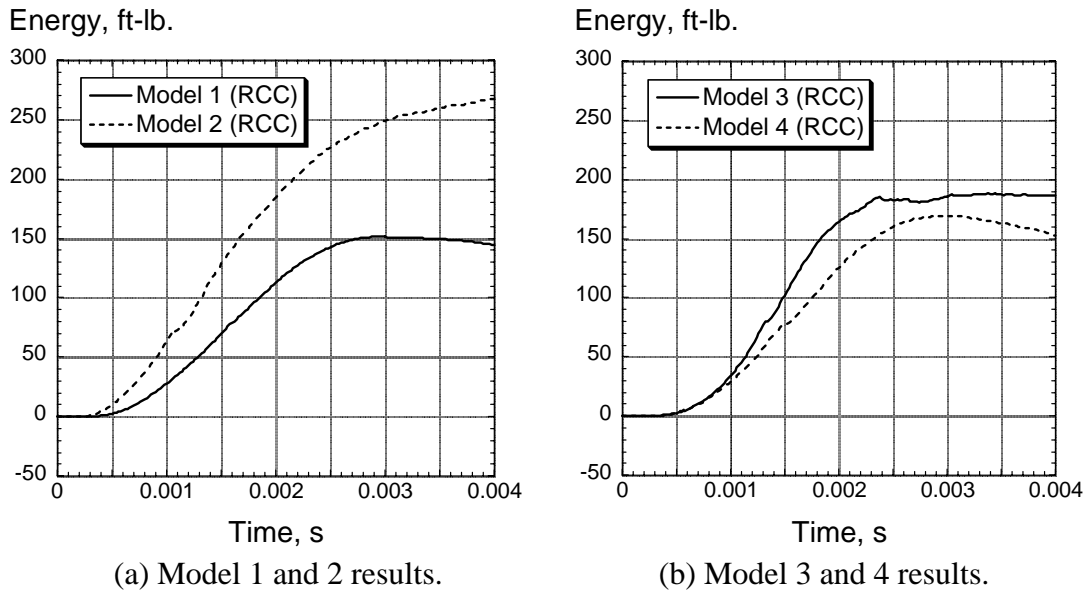
Figure 15. Time-history responses of the internal energy of the RCC.

13

(a) Foam block 1 and 2 results.　　　　(b) Foam block 3 and 4 results.
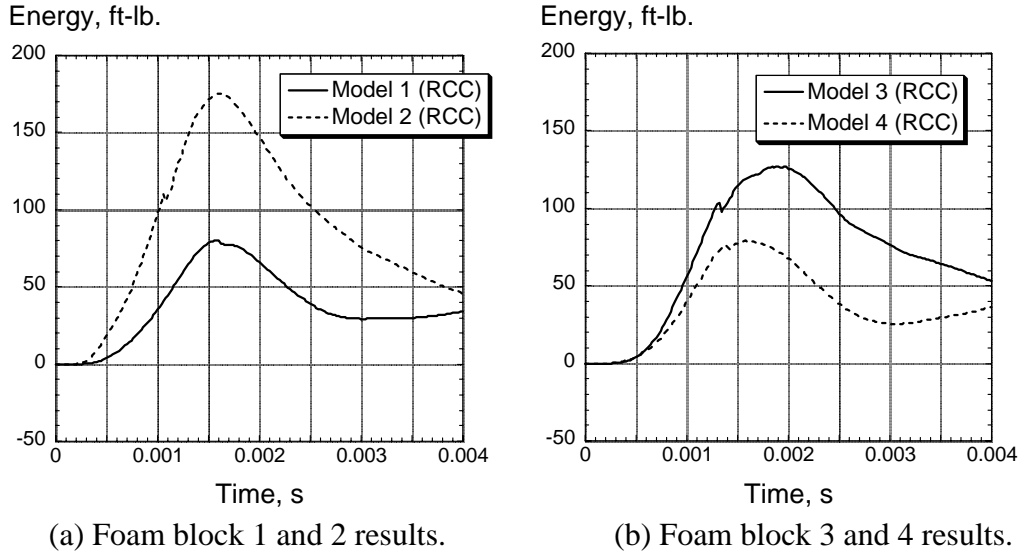
Figure 16. Time-history responses of the kinetic energy of the RCC.

Table 1. Comparison of the number of deleted shell and solid elements in each model at four discrete time steps.

	Model 1 (corner)	Model 2 (long edge)	Model 3 (corner)	Model 4 (short edge)
Estimated damage area, in^2	14.5	39.8	38.6	28.7
Impulse, lb-s	3.91	4.74	4.65	3.85
Max internal energy of the RCC panel, ft-lb.	151.6	267.3	185.4	170.0

Discussion of Results

From the results of this study it was demonstrated that the clocking angle of the projectile is an important factor in determining the amount of damage sustained by the shuttle leading edge RCC panel 9. For this study, the difference was between a small hole in model 1 to large, gaping holes in models 2 and 3. The amount of damage was estimated from the contour plots of first principal infinitesimal strain, shown in Figures 7-10. Based on this analysis, model 2, in which the foam impacts the panel on the middle of the 7-in.-long edge, is the most severe case, since the maximum amount of damage is done to the panel. This model also exhibits the maximum value of internal energy, the maximum contact force, and the highest value of impulse.

It was noted several times that the time history responses of model 2 are quite different when compared with the other three models. A partial explanation may be obtained by examining Figure 17, which shows a side view of the panel models for three time steps immediately following foam impact. For models 1 and 3 the foam impacts the panel on the corner. Also, even though for model 4 the foam impacts the panel along the middle of the 2-in.-long edge, the foam impact for this model behaves very much like a corner impact. It is apparent in Figure 17 that the initial impact of the foam for model 2, in

14

which only the 7-in.-long edge of the foam is in contact initially, is much different from the other cases.
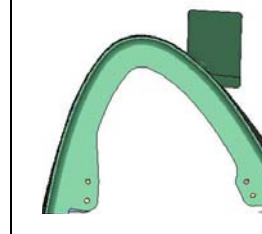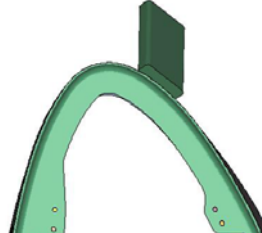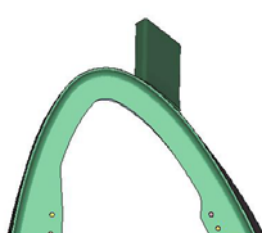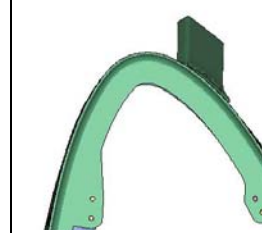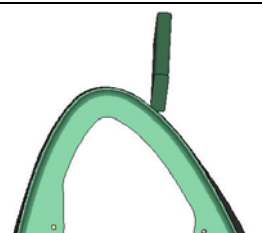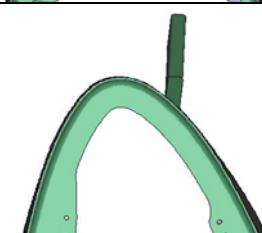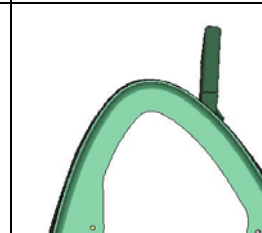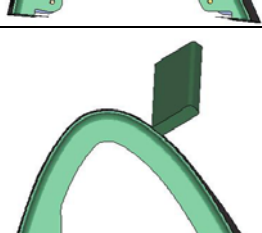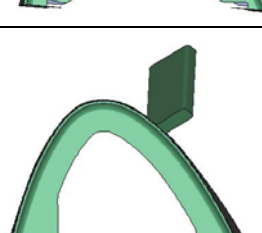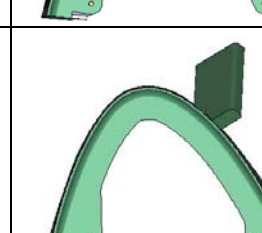
Model	T=0.0002 s	T=0.0004 s	T=0.0006 s
1 (corner)			
2 (long edge)			
3 (corner)			
4 (short edge)			

Figure 17. Model deformations at .0002, .0004, and .0006 seconds showing the initial impact of the foam projectile.

Concluding Remarks

An analytical study was conducted to determine the influence of clocking angle of the projectile on the impact response of space shuttle leading edge wing Panel 9. The foam projectile, a 2-in. x 7 –in. x 11.88-in. rectangular block weighing 0.23-lb., was rotated about its longitudinal axis by 45° and then repositioned such that impact with the panel occurred at the same location (104) on the top surface of the panel. Four different clocking angles were studied. The panels, which are constructed of multiple layers of reinforced carbon carbon (RCC) composite fabric, were represented using material type 58 in LS-DYNA. Likewise, the BX-250 foam was assigned material properties using

material type 83 that included bimodular material behavior and strain rate effects. Of the four simulations performed, two of the foam projectiles initially impacted the panel on the corner of the foam (models 1 and 3); one foam projectile initially impacted the panel on the middle of the 7-in.-long edge (model 2); and one foam projectile impacted the panel on the middle of the 2-in.-long edge (model 4). The simulations were executed in LS-DYNA v. 970 for 4 ms of simulation time.

The results of this study indicate that the clocking angle of the projectile is an important factor in determining the amount of damage sustained by the shuttle leading edge RCC panels. For this study, the difference was between a small hole in model 1 to large, gaping holes in models 2 and 3. It was determined that the most severe case was for model 2, in which the foam initially impacts the panel on the middle of the 7-in.-long edge, since this model exhibited the largest amount of damage, and had the highest impulse and the maximum internal energy of the RCC.

References

1. Gehman, H. W., et al, "Columbia Accident Investigation Board," Report Volume 1, U. S. Government Printing Office, Washington, DC, August 2003.

2. Anon., "LS-DYNA Keyword User's Manual Volume I and II – Version 960," Livermore Software Technology Company, Livermore, CA, March 2001.

3. Carney, K., Melis, M., Fasanella, E., Lyle, K, and Gabrys, J.: "Material Modeling of Space Shuttle leading edge and External Tank Materials for Use in the Columbia Accident Investigation." Proceedings of 8th International LS-DYNA User's Conference, Dearborn, MI, May 2-4, 2004.

4. Melis, M.; Carney, K.; Gabrys, J.; Fasanella, E.; and Lyle, K.: "A Summery of the Space Shuttle Columbia Tragedy and the Use of LS-DYNA in the Accident Investigation and Return to Flight Efforts." Proceedings of 8th International LS-DYNA User's Conference, Dearborn, MI, May 2-4, 2004.

5. Gabrys, J.; Schatz, J.; Carney, K.; Melis, M.; Fasanella, E.; and Lyle, K.: "The Use of LS-DYNA in the Columbia Accident Investigation." Proceedings of 8th International LS-DYNA User's Conference, Dearborn, MI, May 2-4, 2004.

6. Lyle, K.; Fasanella, E.; Melis, M.; Carney, K.; and Gabrys, J.: "Application of Non-Deterministic Methods to Assess Modeling Uncertainties for Reinforced Carbon-Carbon Debis Impacts." Proceedings of 8th International LS-DYNA User's Conference, Dearborn, MI, May 2-4, 2004.

7. Fasanella, E. L., Lyle, K. H., Gabrys, J., Melis, M., and Carney, K., "Test and Analysis Correlation of Foam Impact onto Space Shuttle Wing leading edge RCC Panel 8," Proceedings of 8th International LS-DYNA User's Conference, Dearborn, MI, May 2-4, 2004.

REPORT DOCUMENTATION PAGE

1. REPORT DATE *(DD-MM-YYYY)*	2. REPORT TYPE	3. DATES COVERED *(From - To)*
01- 03 - 2005	Technical Memorandum	

4. TITLE AND SUBTITLE

The Influence of Clocking Angle of the Projectile on the Simulated Impact Response of a Shuttle Leading Edge Wing Panel

5a. CONTRACT NUMBER

5b. GRANT NUMBER

5c. PROGRAM ELEMENT NUMBER

6. AUTHOR(S)

Jackson, Karen E.; Fasanella, Edwin L.; Lyle, Karen H.; and Spellman, Regina L.

5d. PROJECT NUMBER

5e. TASK NUMBER

5f. WORK UNIT NUMBER

23-376-70-30-07

7. PERFORMING ORGANIZATION NAME(S) AND ADDRESS(ES)

NASA Langley Research Center
Hampton, VA 23681-2199

U.S. Army Research Laboratory
Vehicle Technology Directorate
NASA Langley Research Center
Hampton, VA 23681-2199

8. PERFORMING ORGANIZATION REPORT NUMBER

L-19098

9. SPONSORING/MONITORING AGENCY NAME(S) AND ADDRESS(ES)

National Aeronautics and Space Administration
Washington, DC 20546-0001
and U.S. Army Research Laboratory
Adelphi, MD 20783-1145

10. SPONSOR/MONITOR'S ACRONYM(S)

NASA

11. SPONSOR/MONITOR'S REPORT NUMBER(S)

NASA/TM-2005-213538 ARL-TR-3447

12. DISTRIBUTION/AVAILABILITY STATEMENT

Unclassified - Unlimited
Subject Category 05
Availability: NASA CASI (301) 621-0390

13. SUPPLEMENTARY NOTES
An electronic version can be found at http://ntrs.nasa.gov

14. ABSTRACT

An analytical study was conducted to determine the influence of clocking angle of a foam projectile impacting a space shuttle leading edge wing panel. Four simulations were performed using LS-DYNA. The leading edge panels are fabricated of multiple layers of reinforced carbon-carbon (RCC) material. The RCC material was represented using Mat 58, which is a material property that can be used for laminated composite fabrics. Simulations were performed of a rectangular-shaped foam block, weighing 0.23-lb., impacting RCC Panel 9 on the top surface. The material properties of the foam were input using Mat 83. The impact velocity was 1,000 ft/s along the Orbiter X-axis. In two models, the foam impacted on a corner, in one model the foam impacted the panel initially on the 2-in.-long edge, and in the last model the foam impacted the panel on the 7-in.-long edge. The simulation results are presented as contour plots of first principal infinitesimal strain and time history plots of contact force and internal and kinetic energy of the foam and RCC panel.

15. SUBJECT TERMS

Impact simulation; Influence of orientation; Foam projectile; Space shuttle; LS-DYNA

16. SECURITY CLASSIFICATION OF:			17. LIMITATION OF ABSTRACT	18. NUMBER OF PAGES	19a. NAME OF RESPONSIBLE PERSON
a. REPORT	b. ABSTRACT	c. THIS PAGE			STI Help Desk (email: help@sti.nasa.gov)
U	U	U	UU	21	19b. TELEPHONE NUMBER *(Include area code)* (301) 621-0390